JOURNAL OF SOLID STATE CHEMISTRY 44, 32–40 (1982)

The "Pentagonal Column" as a Building Unit in Crystal and Defect Structures of Some Groups of Transition Metal Compounds*

MONICA LUNDBERG, MARGARETA SUNDBERG, AND ARNE MAGNÉLI

Arrhenius Laboratory, University of Stockholm, S-106 91 Stockholm, Sweden

Received November 4, 1981

The pentagonal column (PC) contains MX_7 bipyramids that share their equatorial edges with five MX_6 octahedra. Such groups are linked by their X vertices to form the one-dimensional infinite PC. This structure element appears rather frequently in transition metal oxides and related compounds. In the article use is made of PCs and aggregates of PCs to describe crystal structures and structural defects of such compounds.

Introduction

Structural studies conducted over several decades by means of X-ray diffraction techniques, and later on by high-resolution electron microscopy, have demonstrated the extraordinary wealth of structural variability in transition metal oxide chemistry. The phenomenon called crystallographic shear (*CS*), observed in a large number of partly reduced transition metal oxides, has been widely applied to describe and systematize such compounds as well as ternary oxides containing two metals in different states of oxidation. Most *CS* structures contain just one kind of metal–nonmetal polyhedra, normally with six X atoms octahedrally surrounding an M atom. There are also instances, however, of reduced or mixed oxides containing two polyhedral species, e.g., MX_6 octahedra and MX_4 tetrahedra in several molybdenum and niobium oxide systems.

The structure element discussed in this article contains two kinds of coordination polyhedra, viz., MX_6 octahedra and MX_7 pentagonal bipyramids. The MX_7 bipyramid shares its equatorial edges with five MX_6 octahedra to form groups of the kind illustrated in Fig. 1. Such groups are linked by their X vertices to form one-dimensional infinite strings, conveniently called pentagonal columns (*1*) or PCs for short. This element has been found in the crystal structures of a considerable number of transition metal oxides, oxide fluorides, and oxide hydroxides, and also in connection with structural defects in such compounds. The present article, which is by no means exhaustive, is intended to illustrate how to extend the usefulness of the PC concept as a complement to the several other and related geometrical ways of structure description that have been applied over the years (e.g., (*2–4*)).

Structures Built of PCs Only

Two kinds of structural framework are

* Dedicated to Professor A. F. Wells on his 70th birthday.

0022-4596/82/100032-09$02.00/0

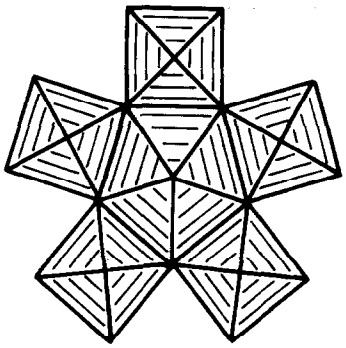

FIG. 1. Repeat unit of the pentagonal column.

known, which are built up exclusively of PCs. In both structures they are linked by corner sharing, i.e., by having outward X atoms in common (Fig. 2). In the Li $Nb_6O_{15}F$ structure the columns are linked in such a way as to form infinite three- and four-sided tunnels parallel to the PC direction (*5*). In $NaNb_6O_{15}F$ the coupling of the columns is different and leads to the creation of three-, four-, and five-sided tunnels (*6*). The alkali atoms are situated in cavities associated with the tunnels in the $Nb_6O_{15}F$ framework. The difference in structure between the lithium and sodium compounds is likely to be associated with the different space requirements of the two alkali metals.

The various possible ways of linking PCs is illustrated in Fig. 3 (*1*). In all four cases, which for obvious reasons may be called edge link, triangle link, diamond link, and corner link, the X atoms involved in the linking are shared between two MX_6 octahedra. The mode of linking therefore does not affect the composition of the resulting atomic aggregate. With this background the $LiNb_6O_{15}F$ structure may be described as composed of corrugated slabs of PCs which are joined among themselves by diamond links (Fig. 4a). Alternatively the structure may be described as composed of straight slabs of PCs joined by triangle links (Fig. 4b). The structure of $NaNb_6O_{15}F$ may also be looked upon as containing straight slabs of PCs. By comparison with the corresponding description of the lithium compound structure, every second slab appears in the reverse direction, which gives rise to the five-sided tunnels in the sodium compound (Fig. 4c). Further possibilities of structures exclusively containing PCs may be imagined, in particular if edge links are

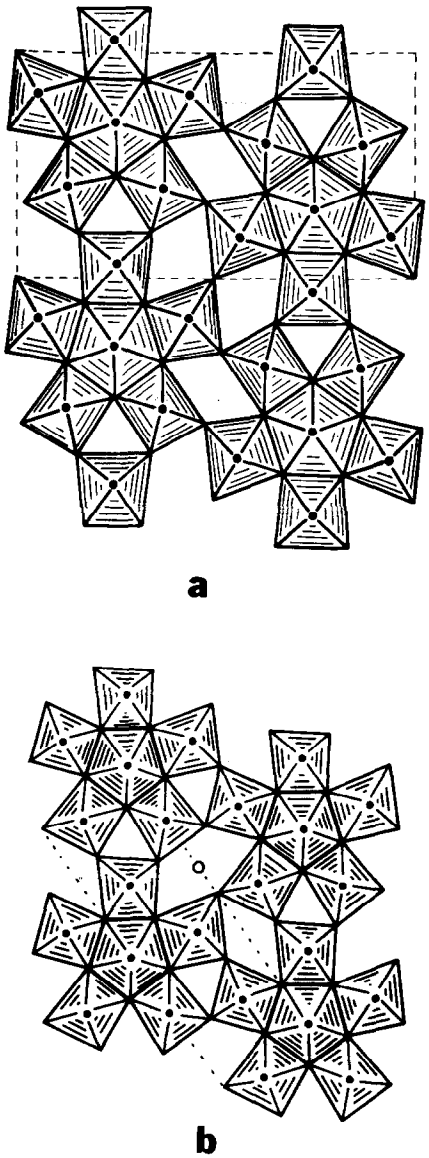

FIG. 2. Framework of PCs in the crystal structures of $LiNb_6O_{15}F$ (a) and $NaNb_6O_{15}F$ (b).

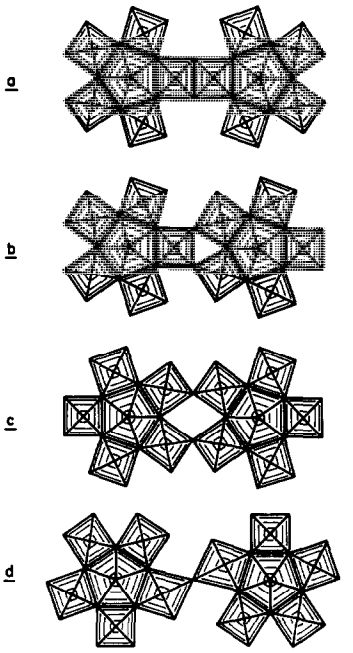

FIG. 3. Different modes of linking PCs, referred to as edge link (a), triangle link (b), diamond link (c), and corner link (d).

taken into consideration (*1*). So far, no such structures seem to have been observed.

While the $NaNb_6O_{15}F$ structure type so far has been observed only for a few compounds, a considerable number of phases are known to belong to the $LiNb_6O_{15}F$ type. These include instances of different occupancy and of substitution at the tunnel atom sites, as well as substitution of the metal and nonmetal atoms in the framework of PCs, e.g., Ta_3O_7F (*7*), Nb_2WO_8 (*8*), high-$LiTa_3O_8$ (*9, 10*), and $Cu_{0.8}Ta_3O_8$ (*11*). Deviations from the *Pmma* symmetry of Li $Nb_6O_{15}F$ are frequently met in such compounds, which may also exhibit superstructures. This is likely to be essentially due to puckering of the *M* atom layers normal to the PC direction.

PCs Combined with Other Structure Elements

The PC unit bears an interesting relationship to the tetragonal tungsten bronze structure (TTB), first determined for the compound K_xWO_3 (Fig. 5a). This contains a framework of WO_6 octahedra linked by corners in such a way as to form infinite three-, four-, and five-sided tunnels, the alkali atoms being situated in the two wider types of tunnels (*12, 13*). In the Nb_2O_5–WO_3 and Ta_2O_5–WO_3 systems phases exist with structures rather similar to the TTB structure. In such phases, with an oxygen-

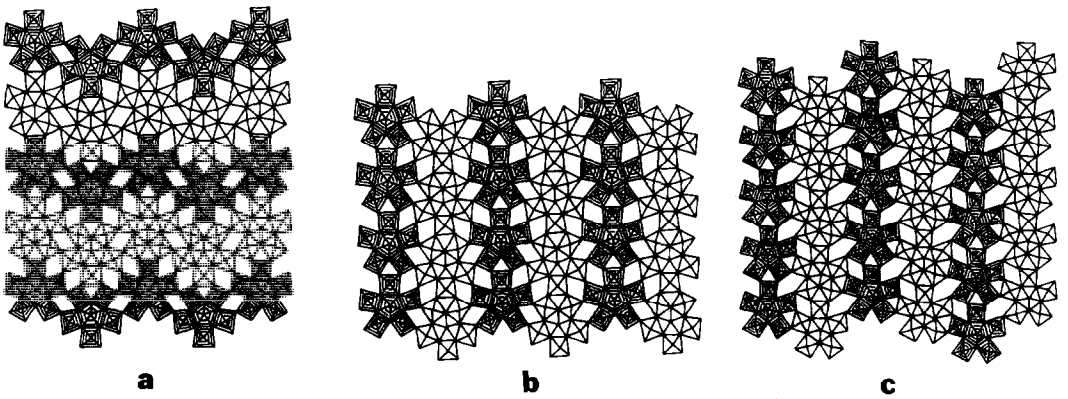

FIG. 4. Structure of $LiNb_6O_{15}F$ described as composed of corrugated slabs of diamond-linked PCs (a) and of straight slabs of triangle-linked PCs (b). Structure of $NaNb_6O_{15}F$ illustrated as composed of straight slabs of triangle-linked PCs (c). The arrangements in (b) and (c) differ with respect to the mutual orientation of adjacent slabs.

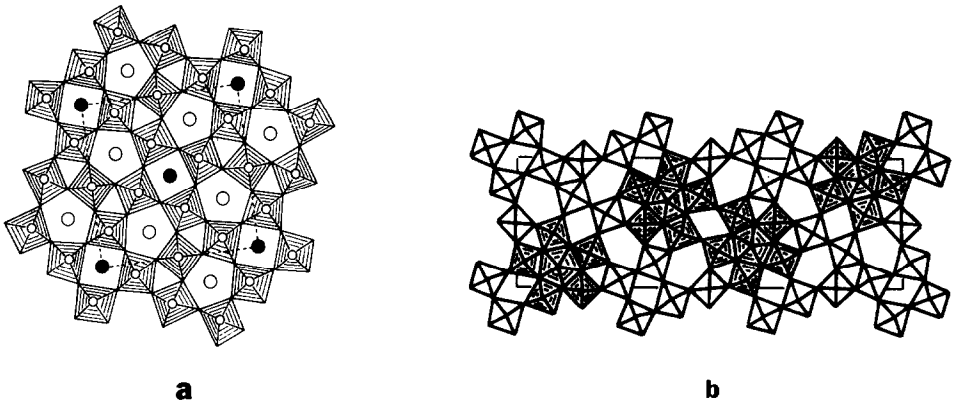

FIG. 5. Framework of tetragonal tungsten bronze (TTB) structure (a). Structure of $Nb_8W_9O_{47}$ (b). The unit cell of the latter is three times the size of the TTB cell and 4 out of 12 of the pentagonal tunnels are filled with metal and oxygen atoms and thus transformed into PCs.

to-transition metal ratio lower than the value of 3 of the tungsten bronze, the compositional deviation is resolved by equal numbers of metal and oxygen atoms entering pentagonal tunnels of a TTB-type framework. The insertion of atoms transforms the pentagonal tunnel, or rather pentagonal tube of five MO_6 octahedra (PT), of the bronze into a PC. The crystal structure of $Nb_8W_9O_{47}$ (*14*) has a unit cell three times the size of the TTB cell, and 4 out of the 12 PTs are filled with metal and oxygen atoms and thus transformed into PCs, which are distributed in an ordered way (Fig. 5b).

A rotation mechanism has been devised (*15, 16*) which in a simple way demonstrates a relationship between the TTB and the ReO_3-type structures (Fig. 6). If, in the latter, square groups of four MX_6 octahedra, or rather infinite tetragonal tubes composed of such groups, are rotated by $\pi/4$ radians, an atomic arrangement with the characteristic three-, four-, and five-sided tunnels of the TTB structure is formed. This implies that PTs may fit coherently into an ReO_3-type structure, and so may also a PC. From this point of view the structure of $Nb_8W_9O_{47}$ may be described as an ordered arrangement of pairs of PCs in an ReO_3-type matrix. The components of the double columns are mutually joined by diamond links. In $Nb_4W_7O_{31}$ (*17*) double PCs occur in a more diluted, ordered arrangement in the WO_3 matrix. A large number of related intermediary phases and pseudophases with varying degrees of order have been found in the Nb_2O_5–WO_3 system (*18*).

The geometrical relations within this group of structures may be further extended in the following way. An alternative description of the TTB structure is in terms of slabs of diamond-linked PTs running along the (110) (and $(1\bar{1}0)$) directions. The slabs are linked by a network of WO_6 octahedra (Fig. 7a). If the nonshaded groups of octahedra are shifted by $a/2^{1/2}$ along the face diagonal of the cell, two out of four

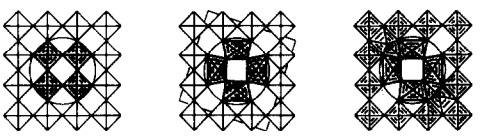

FIG. 6. Relation between ReO_3 type and TTB structure. Rotation of square unit of four octahedra indicated in (a) by $\pi/4$ radians leads to formation of three- and five-sided tunnels characteristic of the TTB structure (b). Two five-sided tunnels filled with metal and oxygen atoms to become two diamond-linked PCs (c).

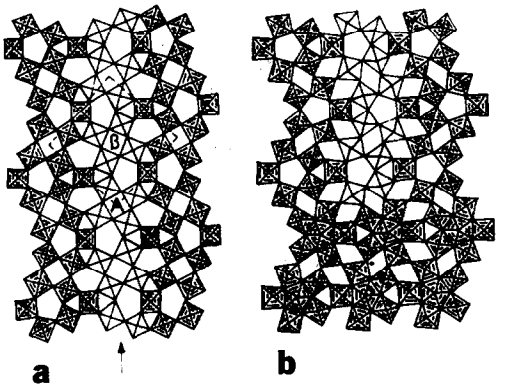

FIG. 7. Geometrical relation between the TTB and $LiNb_6O_{15}F$ structures. (a) TTB described as composed of slabs of pentagonal tubes (PT) and MX_6 octahedra. (b) $LiNb_6O_{15}F$ framework derived from (a) by shifting nonshaded MX_6 octahedra by $a/2^{1/2}$ and (in lower part of figure) completing remaining PTs to become PCs.

five-sided tunnels are transformed into diamond-shaped ones (Fig. 7b). The arrangement of octahedra thus formed is analogous to that of the structure of $LiNb_6O_{15}F$. By filling all the PTs with M and X atoms the framework of PCs is obtained.

In the structure of Mo_5O_{14} (*19*) only single PCs are present, distributed in such a way as to create not only three-, four-, and five-sided tunnels but also six-sided ones. This is illustrated in a very clear way by applying the rotation mechanism (*16*). An alternative way of describing the structure is given below.

Hexagonal tunnels (HT) are also present in the structure of $W_{18}O_{49}$ (*20*) (Fig. 8). Here, doublets of edge-linked PCs are joined by diamond links to form infinite slabs. These are in turn mutually linked via an arrangement of corner-sharing WO_6 octahedra. The edge-linked pair of columns is not compatible with an ReO_3-type matrix, and the atomic arrangement of the structure becomes a rather irregular one. In this connection it is of interest to observe that high-resolution electron microscopy (HREM) studies have shown structural defects to occur very rarely in $W_{18}O_{49}$ as compared to similar ReO_3-compatible structures (*21*). The $W_{18}O_{49}$ structure will be further commented on below.

The structure of $Mo_{17}O_{47}$ (*22*) may be described as containing isolated doublets of edge-linked PCs. The arrangement of corner-sharing MoO_6 octahedra between the columns is quite irregular, and the structure is not compatible with the ReO_3 type.

The crystal structure of a new tungsten oxide (*23*) has recently been derived from HREM images (Fig. 9a). Its formula, which has so far been given as the unit cell content $W_{24}O_{68}$, will, for structural reasons presented below, be expressed as $W_{12}O_{34}$. The sample used for the structural work was not single phase and was in a poor state of crystallinity, giving quite unsatisfactory X-ray powder photographs. In spite of this, electron-diffraction patterns as well as electron micrographs were of fairly good quality. (It should be added that recent work on the mechanism of formation and defect structure of the oxide also includes improved methods for synthesis (*24*).) The structure (Fig. 10) may be described as an ordered intergrowth of corrugated slabs of diamond-linked PCs (cf. Fig. 4a) and slabs of WO_3. Structural defects due to deviating thickness of the WO_3 slabs have occasionally been observed in the images (A in Fig. 9a). The electron-diffraction pattern, how-

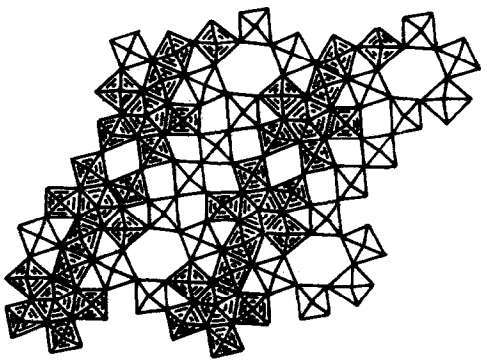

FIG. 8. Structure of $W_{18}O_{49}$ viewed along the short axis.

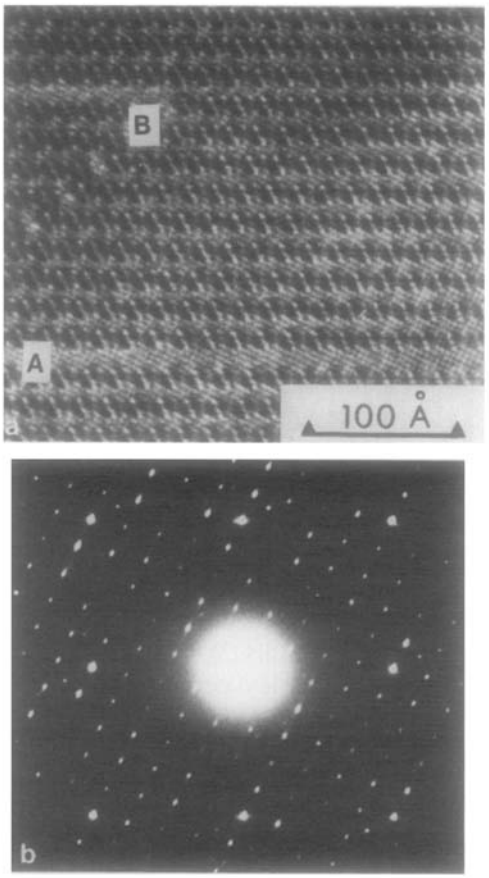

FIG. 9. (a) HREM image of a thin crystal fragment of $W_{12}O_{34}$. Interpretation is given in Fig. 10. Defects at A and B are described in the text. (b) Electron diffraction pattern of $W_{12}O_{34}$.

ever, in all cases has the character illustrated in Fig. 9b. The strongest reflections indicate the presence of a WO_3 substructure, with sharp superstructure reflections showing an 11-fold periodicity in the [102] direction.

The character of the diffraction pattern is rather reminiscent of those of the members of the homologous series of *CS* phases in the molybdenum and tungsten oxide systems. The slabs of PCs in $W_{12}O_{34}$ would thus correspond to the two-dimensional arrangement of edge-linked octahedra in the *CS* structures, which are regularly spaced in the ReO_3-type matrix at distances given by the value of n in the formulae of the respective homologous series. It should be observed, however, that the *CS* mechanism introduces an out-of-step component in the ReO_3 matrix, while the PC on the other hand is compatible with the matrix. This is illustrated by the occurrence of terminating PC slabs in $W_{12}O_{34}$ (B in Fig. 9a). The appearance of the image clearly shows coherence of the WO_3 pattern surrounding the end of such slabs. This is in contrast with the blurred character of the WO_3 areas observed around terminating *CS* planes.

In order to express the structural character of $W_{12}O_{34}$ its formula may be written $(WO_3)_5WO(WO_3)_{11-5}$. This should in turn correspond to the five WO_6 octahedra of the pentagonal tunnel, the inserted atoms which transform the PT into a PC, and the WO_3 slab atoms. The number 11 corresponds to the number of WO_6 octahedra between the WO_7 bipyramids (cf. Fig. 10) and also to the periodicity of the superstructure.

A homologous series built on the structural principles found in $W_{12}O_{34}$ is easily imaginable. It would take the general formula $(MO_3)_5MO(MO_3)_{n-5}$. The low-end member ($n = 5$) of the series is the structure composed solely of slabs of diamond-linked PCs, i.e., the framework of $LiNb_6$

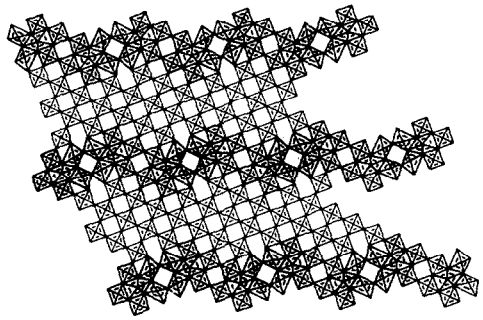

FIG. 10. Idealized structure model of $W_{12}O_{34}$ derived from lattice image. Corrugated slabs of diamond-linked PCs (drawn with heavy lines and extended to the right) alternate with slabs of WO_3. The direction of the characteristic width of the slabs (n value in formula of homologous series) is indicated.

$O_{15}F$. High members of the series are represented by the mixed oxides $4Nb_2O_5 \cdot 22WO_3$ and $4Nb_2O_5 \cdot 50WO_3$ (*25*). The crystal structures derived from HREM images may be interpreted as composed of slabs of diamond-linked PCs intergrown with WO_3 slabs, in full analogy with the $W_{12}O_{34}$ structure. If M represents both metals, the formulae may be written $(MO_3)_5 MO(MO_3)_{14-5}$ and $(MO_3)_5MO(MO_3)_{28-5}$. This would indicate superstructures of periodicity 14 and 28, respectively, and such superstructure reflections actually seem to be present in the electron diffractogram in Ref. (*25*).

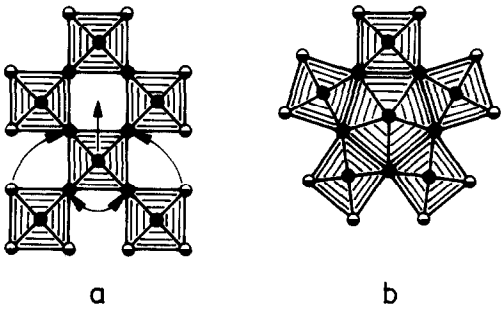

FIG. 12. Formation of a PC (b) from six WO_6 octahedra (a). The process involves elimination of two oxygen atoms.

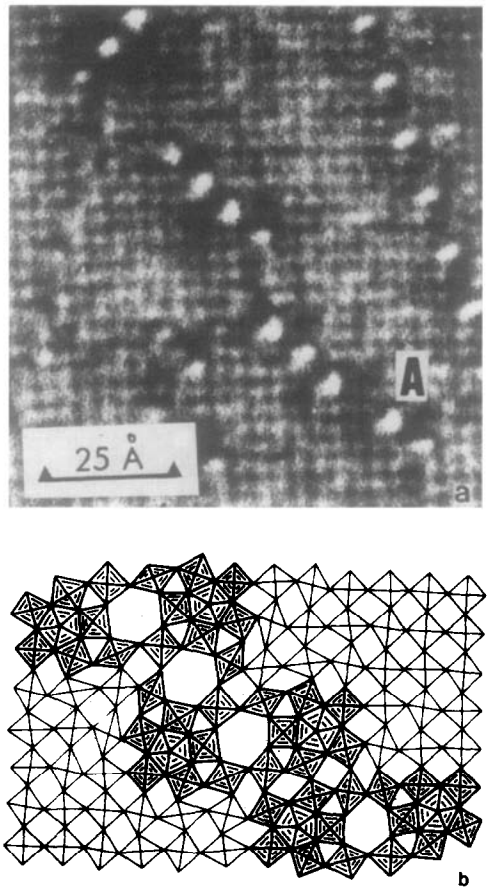

FIG. 11. (a) HREM image of thin crystal of $WO_{2.90}$ showing {103} *CS* to the right and zig-zag rows of black dots and white spots (PC–HT defects) at A. (b) Interpretation of the area around A, also showing a mistake in the PC–HT defect, viz., direct corner link between two PCs.

PCs in Defect Structures

HREM studies on slightly reduced tungsten trioxide crystals ($WO_{2.98}$) (*26*) show, in addition to Wadsley defects consisting of grossly disordered {102} *CS* planes, "star-shaped" defects within the areas of nonreduced WO_3 slabs. Mostly the stars occur isolated, but occasionally they appear in rows running parallel to the *CS* planes. The images obviously show the projections of a new kind of linear defect. Arguments based on the size, shape, and contrast of the stars and on the similarity with the images given by $W_{12}O_{34}$ suggest that these defects consist of pairs of PCs mutually joined by diamond

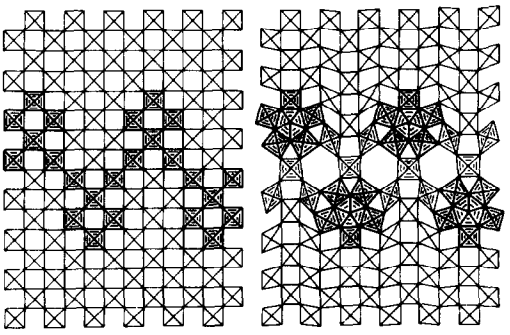

FIG. 13. Formation of the PC–HT defect from the WO_3 network.

links, as illustrated in Fig. 6c (*27*). The same kind of double PCs is also present in $Nb_8W_9O_{47}$ (Fig. 5b). The new type of one-dimensional defect suggested here is compatible with the WO_3 structure.

Another type of structural defect involving PCs has been observed in reduced tungsten trioxide, both in the WO_3 areas and in connection with {102} and {103} *CS* (*28*), and also in intergrowth tungsten bronzes (ITB) (*29*). This is illustrated in Fig. 11a, which shows a micrograph of a thin crystal fragment of composition $WO_{2.90}$. Major portions of the image (not shown in the figure) exhibit fairly well-ordered {103} *CS*. The defects are visible in the figure as zig-zag rows of black dots and white spots. The latter are all arranged linearly at angles of 45° to the WO_3 matrix. An interpretation of the defect arrangement is given in Fig. 11b. It may be described as PCs alternating with hexagonal tunnels (HT) to form the zig-zag rows. The figure also contains an instance of a mistake in the PC–HT defect, viz., two PCs joined directly by a corner link.

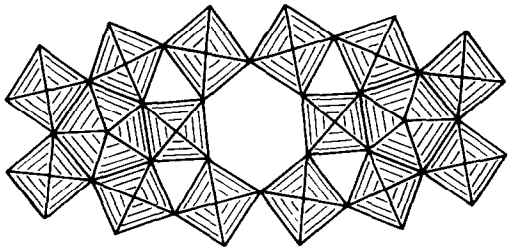

FIG. 14. PC–HT–PC group.

The occurrence of PC–HT defects under conditions similar to those which give rise to shear structures suggests that one should be able to derive the new type of defect from the ReO_3 network by elimination of oxygen atoms and a slight collapse of the basic WO_3 structure. A possible geometric model for this mechanism, illustrated in projection in Figs. 12 and 13, shows how groups of six WO_6 octahedra, after elimination of two oxygen atoms, are rearranged to form a PC unit, and how the zig-zag rows of alternating PCs and HTs line up in [101] directions of the WO_3 matrix.

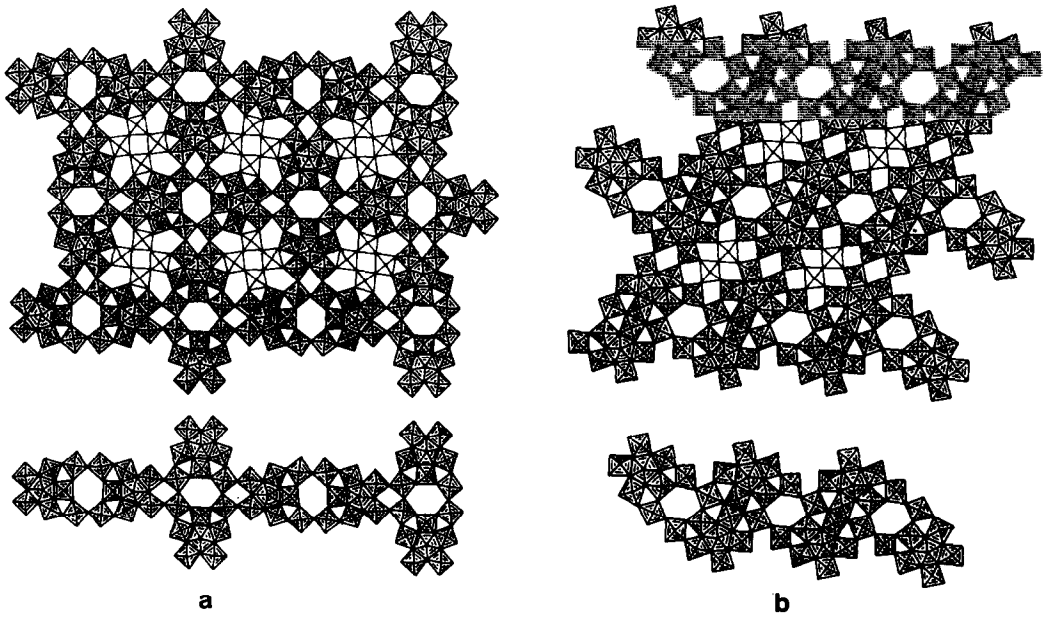

FIG. 15. Structures of Mo_5O_{14} (a) and $W_{18}O_{49}$ (b) described in terms of PC–HT–PC units.

PC–HT–PC as a Structure Element

The PC–HT–PC group (Fig. 14) characteristic of the defect structure described above has also been found useful for description of the complicated structures of Mo_5O_{14} and $W_{18}O_{49}$. This should be obvious from Fig. 15. In Mo_5O_{14} all except 8 of the 40 polyhedra that make up the unit cell may be associated with a network of corner-sharing PC–HT–PC units. The remaining eight MoO_6 octahedra are linked by corners in the ReO_3 way to form infinite strings, which fill the space between the PC–HT–PC groups.

In $W_{18}O_{49}$, only 2 WO_6 octahedra out of 18 polyhedra do not fit into PC–HT–PC units. As mentioned above, the linking between the PC units involves edge sharing. The structure may therefore be alternatively described as built up of slabs of roof-tile stacked PC–HT–PC units. The slabs are joined by diamond links and pairs of WO_6 octahedra.

Acknowledgments

Valuable discussions with Professor Lars Kihlborg, Dr. Bengt-Olov Marinder, and Mr. Wubeshet Sahle are gratefully acknowledged. The work has been supported by the Swedish Natural Science Research Council.

References

1. M. LUNDBERG, *Chem. Commun. Univ. Stockholm*, No. XII (1971).
2. B. G. HYDE, A. N. BAGSHAW, S. ANDERSSON, AND M. O'KEEFFE, *Annu. Rev. Mater. Sci.* **4**, 43 (1974).
3. T. EKSTRÖM, *Chem. Commun. Univ. Stockholm*, No. VII (1975).
4. T. EKSTRÖM AND R. J. D. TILLEY, *Chem. Scr.* **16**, 1 (1980).
5. M. LUNDBERG, *Acta Chem. Scand.* **19**, 2274 (1965).
6. S. ANDERSSON, *Acta Chem. Scand.* **19**, 2285 (1965).
7. L. JAHNBERG AND S. ANDERSSON, *Acta Chem. Scand.* **21**, 615 (1967).
8. M. LUNDBERG, *Acta Chem. Scand.* **26**, 2932 (1972).
9. A. G. NORD AND J. O. THOMAS, *Acta Chem. Scand. A* **32**, 539 (1978).
10. G. D. FALLON, B. M. GATEHOUSE, R. S. ROTH, AND S. A. ROTH, *J. Solid State Chem.* **27**, 255 (1979).
11. P. NDALAMBA WA ILUNGA, B. O. MARINDER, AND M. LUNDBERG, *Chem. Scr.* **18**, 217 (1981).
12. A. MAGNÉLI, *Ark. Kemi* **1**, 213 (1949).
13. L. KIHLBORG AND A. KLUG, *Chem. Scr.* **3**, 207 (1973).
14. A. SLEIGHT, *Acta Chem. Scand.* **20**, 1102 (1966).
15. L. A. BURSILL AND B. G. HYDE, *Nature (London) Phys. Sci.* **240**, 122 (1972).
16. B. G. HYDE AND M. O'KEEFFE, *Acta Crystallogr. A* **29**, 243 (1973).
17. S. IIJIMA AND J. G. ALLPRESS, *Acta Crystallogr. A* **30**, 22 (1974).
18. H. OBAYASHI AND J. S. ANDERSON, *J. Solid State Chem.* **17**, 79 (1976).
19. L. KIHLBORG, *Ark. Kemi* **21**, 427 (1963).
20. A. MAGNÉLI, *Ark. Kemi* **1**, 223 (1949).
21. W. SAHLE, *J. Solid State Chem.*, in press.
22. L. KIHLBORG, *Acta Chem. Scand.* **14**, 1612 (1960); **17**, 1485 (1963).
23. M. SUNDBERG, *Chem. Scr.* **14**, 161 (1978–79).
24. W. SAHLE AND M. SUNDBERG, in preparation.
25. S. IIJIMA, *Acta Crystallogr. A* **34**, 922 (1978).
26. M. SUNDBERG AND R. J. D. TILLEY, *J. Solid State Chem.* **11**, 150 (1974).
27. M. SUNDBERG, *Chem. Commun. Univ. Stockholm*, No. 5 (1981).
28. W. SAHLE AND M. SUNDBERG, *Chem. Scr.* **16**, 163 (1980).
29. L. KIHLBORG, M. SUNDBERG, AND A. HUSSAIN, *Chem. Scr.* **15**, 182 (1980).